

# Construction of a Gyrokinetic Plasma Simulation Model for Electromagnetic Phenomena

Yasushi TODO and Atsushi ITO

*National Institute for Fusion Science, Toki 509–5292, Japan*

(Received 16 March 2007 / Accepted 10 April 2007)

A new gyrokinetic plasma simulation model for electromagnetic phenomena is presented. In this model, the total characteristic method, where the  $\delta f$  particle-in-cell simulation model is complemented with the fluid model to satisfy the conservation properties, is applied to electrons. The electric field component parallel to the magnetic field is calculated from the time derivative of Ampère's law. It is demonstrated that both the real frequency and damping rate of kinetic Alfvén wave are computed correctly for various electron beta values. It is also shown that with respect to the number of marker particles, the numerical convergence of real frequency and damping rate is faster with the total characteristic method than with the conventional  $\delta f$  method. Specifically, it is demonstrated that the total characteristic method enables a simulation of a kinetic Alfvén wave with a grid size ten times larger than the electron skin depth, while the wave damps spuriously for the same physical condition in a conventional  $\delta f$  simulation.

© 2007 The Japan Society of Plasma Science and Nuclear Fusion Research

Keywords: gyrokinetic simulation, electromagnetic plasma phenomenon, total characteristic method,  $\delta f$  particle-in-cell method

DOI: 10.1585/pfr.2.020

## 1. Introduction

The gyrokinetic particle-in-cell (PIC) simulation model is a powerful tool for investigating low frequency microinstabilities in magnetized plasmas [1]. When the fusion core plasmas are simulated with the gyrokinetic PIC method, the  $\delta f$  method [2–5] is often employed to reduce the numerical noise. Electromagnetic phenomena can be simulated with the gyrokinetic model coupled with the Poisson and Ampère equations. The internal kink mode was investigated with the gyrokinetic  $\delta f$  PIC method [6]. A difficulty was suggested in accurately solving Ampère's law with a term in proportion to the inverse square of the electron skin depth, when the gyrokinetic PIC method is applied to electromagnetic phenomena [7, 8]. In order to overcome this difficulty and relax the restriction of the Courant condition for electrons, split-weight schemes of the  $\delta f$  PIC method have been devised [8, 9]. It was also reported that this difficulty could be resolved with a conventional  $\delta f$  scheme with careful normalization applied to the skin terms [10]. In another trend for electromagnetic gyrokinetic simulation, electrons are simulated with a fluid model [11] or with fluid-kinetic hybrid models [12, 13].

The total characteristic method [14] was presented to improve the conservation properties, i.e., the conservation of particles, momentum, and energy, in the  $\delta f$  PIC simulation. In the  $\delta f$  PIC simulation, the distribution function is expressed as the sum of the reference distribution and variation distribution. The PIC model is not applied to the reference distribution, often represented by  $f_0$ , which

is defined in advance of the simulation. Only the variation distribution  $\delta f$  is approximated by the Klimontovich distribution function  $\delta f_K$  using Lagrangian markers (marker particles). The time evolution of  $\delta f_K$  is described by an advection term and a source term associated with  $f_0$ . It was shown that the source term, which is a Monte Carlo estimate in the  $\delta f$  method, violates the conservation properties [14]. In the  $\delta f$  simulation, each Lagrangian marker represents a characteristic of the Vlasov equation. However, the characteristics which the Lagrangian markers do not represent are not considered in the  $\delta f$  simulation. In the total characteristic method, a fluid system provides characteristics complementary to those represented by the Lagrangian markers. The corrections to the Monte Carlo estimate of the source term propagate along the complementary characteristics provided by the fluid system.

In this paper, an electromagnetic gyrokinetic simulation model is presented using the total characteristic method. The new model is described in Sec. 2. In Sec. 3, both the real frequency and damping rate of the kinetic Alfvén wave are demonstrated to compute correctly for various electron beta values. It is shown that with respect to the number of marker particles, the numerical convergence of real frequency and damping rate is faster with the total characteristic method than with the conventional  $\delta f$  method. Specifically, it is demonstrated that the total characteristic method enables a simulation of a kinetic Alfvén wave with a grid size ten times larger than the electron skin depth, while the wave damps spuriously for the same physical condition in the conventional  $\delta f$  simulation. A sum-

author's e-mail: todo@nifs.ac.jp

mary is given in Sec. 4.

## 2. Construction of an Electromagnetic Plasma Model with the Total Characteristic Method

### 2.1 Vlasov-Poisson-Ampère system

We consider phenomena with frequency lower than the ion cyclotron frequency in the uniform magnetic field  $\mathbf{B}_0$ . We express the electromagnetic field using the scalar potential  $\phi$  and the vector potential parallel to the magnetic field  $A_{\parallel}$

$$\mathbf{E} = -\nabla\phi - \mathbf{b}\frac{\partial}{\partial t}A_{\parallel}, \quad (1)$$

$$\mathbf{B} = \mathbf{B}_0 + \nabla \times (A_{\parallel}\mathbf{b}), \quad (2)$$

where  $\mathbf{b} = \mathbf{B}/B$ . The perpendicular components of the vector potential are neglected because we focus on incompressible perturbations of the magnetic field. For the low frequency phenomena, the gyrokinetic model provides a useful physical framework.

When the equilibrium number density and the electron temperature are given by  $n_0$  and  $T_{e0}$ , the Debye length is  $\lambda_D = \sqrt{\epsilon_0 T_{e0}/n_0 e^2}$ . The gyrokinetic Poisson equation in the long wavelength approximation for the electrostatic potential is

$$\left(\frac{\rho_s}{\lambda_D}\right)^2 \nabla_{\perp}^2 \phi = -\frac{q_i n_i + (-e)n_e}{\epsilon_0}, \quad (3)$$

where  $n_i$  and  $n_e$  are the ion and electron number density, and  $q_i$  is the ion charge. In the definition of  $n_i$  and  $n_e$ , the polarization drift effects are not included. The ion polarization charge density is given by the left-hand side of Eq. (3). Thus, Eq. (3) represents the quasi-neutrality condition without the electron polarization charge density. We define  $\rho_s = c_s/\Omega_i$ , where  $c_s = \sqrt{T_{e0}/m_i}$ ,  $\Omega_i = q_i B_0/m_i$ , and  $m_i$  is the ion mass. The operator  $\nabla_{\perp}^2$  is  $\nabla \cdot [\nabla - \mathbf{b}(\mathbf{b} \cdot \nabla)]$ . The Ampère's law for the vector potential is

$$\nabla_{\perp}^2 A_{\parallel} = -\mu_0(j_i + j_e), \quad (4)$$

where  $j_i$  and  $j_e$  are the ion and electron current density parallel to the magnetic field.

The equations of motion for electrons and ions are

$$\dot{\mathbf{x}} = v_{\parallel}\mathbf{b} + \frac{\mathbf{E} \times \mathbf{B}}{B^2}, \quad (5)$$

$$\dot{v}_{\parallel} = \frac{q_{\sigma}}{m_{\sigma}} E_{\parallel} \quad (\sigma = i, e), \quad (6)$$

where  $v_{\parallel}$  is the velocity parallel to the magnetic field. The parallel electric field  $E_{\parallel}$  is needed for the time integration of the equations of motion. The parallel electric field  $E_{\parallel}$  is given from Eq. (1)

$$E_{\parallel} = -\mathbf{b} \cdot \nabla\phi - \frac{\partial}{\partial t}A_{\parallel}. \quad (7)$$

Operating  $\nabla_{\perp}^2$  to Eq. (7) and coupling the resultant equation with the time derivative of Eq. (4), we find that

the parallel electric field is given by the following equation,

$$\nabla_{\perp}^2 E_{\parallel} = -\nabla_{\perp}^2 (\mathbf{b} \cdot \nabla\phi) + \mu_0 \frac{\partial}{\partial t} (j_i + j_e). \quad (8)$$

The distribution function of the guiding-center evolves following the drift kinetic equation ( $\sigma = i, e$ ):

$$\frac{\partial}{\partial t} f_{\sigma} + \left( v_{\parallel}\mathbf{b} + \frac{\mathbf{E} \times \mathbf{B}}{B^2} \right) \cdot \nabla f_{\sigma} + \frac{q_{\sigma} E_{\parallel}}{m_{\sigma}} \frac{\partial}{\partial v_{\parallel}} f_{\sigma} = 0. \quad (9)$$

Finite Larmor radius effects are omitted for simplicity. Equation (9) is multiplied by  $q_{\sigma} v_{\parallel}$  and integrated in the velocity space. This procedure gives the time evolution of the current density on the right-hand-side of Eq. (8)

$$\frac{\partial}{\partial t} j_{\sigma} = -\frac{q_{\sigma}}{m_{\sigma}} \mathbf{b} \cdot \nabla P_{\parallel\sigma} - \frac{\mathbf{E} \times \mathbf{B}}{B^2} \cdot \nabla j_{\sigma} + \frac{n_{\sigma} q_{\sigma}^2}{m_{\sigma}} E_{\parallel}, \quad (10)$$

$$P_{\parallel\sigma} = \int m_{\sigma} v_{\parallel}^2 f_{\sigma} d^3 v. \quad (11)$$

Finally, we obtain the equation for the parallel electric field

$$\left( \nabla_{\perp}^2 - \sum_{\sigma=i,e} \frac{\omega_{p\sigma}^2}{c^2} \right) E_{\parallel} = -\nabla_{\perp}^2 (\mathbf{b} \cdot \nabla\phi) - \sum_{\sigma=i,e} \mu_0 \left( \frac{q_{\sigma}}{m_{\sigma}} \mathbf{b} \cdot \nabla P_{\parallel\sigma} + \frac{\mathbf{E} \times \mathbf{B}}{B^2} \cdot \nabla j_{\sigma} \right), \quad (12)$$

where  $\omega_{p\sigma} = \sqrt{n_{\sigma} q_{\sigma}^2 / \epsilon_0 m_{\sigma}}$ . Equations (1)-(6) and (12) constitute a closed set of the electromagnetic plasma model.

### 2.2 1-dimensional simulation model with the total characteristic method

In this subsection, we construct a 1-dimensional simulation model. The 1-dimensional phase space ( $x, v_{\parallel}$ ) is considered. We assume cold ions with constant number density  $n_0$  and focus on electron dynamics. For cold ions,  $n_i$  does not change in time, because the  $\mathbf{E} \times \mathbf{B}$  drift in the  $x$  direction vanishes in the 1-dimensional model. Note that the ion polarization charge density is considered in the left-hand side of Eq. (3). The equilibrium distribution of electrons is assumed to be a Maxwellian distribution:

$$f_{e0}(x, v_{\parallel}) = \frac{n_0}{\sqrt{2\pi T_{e0}/m_e}} e^{-m_e v_{\parallel}^2 / 2T_{e0}}. \quad (13)$$

We simulated the evolution of the distribution function using the total characteristic method where the  $\delta f$  PIC model is complemented with the fluid model [14]. The position and velocity of Lagrangian markers evolve according to the equation of motion (Eqs. (5) and (6)). The Lagrangian markers were loaded uniformly in the phase space,  $0 \leq x \leq L$ ,  $-5v_t \leq v \leq 5v_t$ , where  $v_t = \sqrt{T_{e0}/m_e}$  and  $L$  is the wavelength to be investigated. The initial velocity of the Lagrangian markers was scrambled with the bit-reversed technique [15]. The probability density of the

Lagrangian markers is uniform  $p(x, v_{\parallel}) = 1/V$ , where  $V$  is the phase space volume and  $V = 10v_t L$ .

The following equation gives the weight evolution of marker particles:

$$\frac{dw_j}{dt} = -\frac{V}{N} \frac{(-e)}{m_e} E_{\parallel}(x_j, t) \frac{n_0}{\sqrt{2\pi}v_t} \left(\frac{-v_j}{v_t^2}\right) e^{-v_j^2/2v_t^2}, \quad (14)$$

$$w_j(t=0) = 0. \quad (15)$$

In the conventional  $\delta f$  simulation, the electron number density, current density, and parallel pressure are estimated using the  $\delta f$  Klimontovich distribution function:

$$n(x, t) = n_0 + \delta n_K(x, t), \quad (16)$$

$$\delta n_K(x, t) \equiv \sum_{j=1}^N w_j S(x - x_j), \quad (17)$$

$$j(x, t) = \delta j_K(x, t), \quad (18)$$

$$\delta j_K(x, t) = \sum_{j=1}^N w_j (-e) v_{\parallel j} S(x - x_j), \quad (19)$$

$$P(x, t) = n_0 T_{e0} + \delta P_K(x, t), \quad (20)$$

$$\delta P_K(x, t) = \sum_{j=1}^N w_j m_e v_{\parallel j}^2 S(x - x_j), \quad (21)$$

where  $S(x - x_j)$  is a shape factor. We should notice that  $n_0$ ,  $j_0$ , and  $T_{e0}$  are constant in space and time. With the total characteristic simulation model, the equations for the number density and current density are derived from Eq. (15) of Ref. [14], while the isothermal model is assumed for the pressure evolution. The following fluid equations are employed in the total characteristic simulation:

$$\begin{aligned} \frac{\partial}{\partial t} \delta n_g(x, t) &= -\frac{b_x}{(-e)} \frac{\partial}{\partial x} \delta j_g(x, t) \\ &\quad - \sum_{j=1}^N \frac{dw_j}{dt} S(x - x_j), \end{aligned} \quad (22)$$

$$\begin{aligned} \frac{\partial}{\partial t} \delta j_g(x, t) &= -\frac{(-e)b_x}{m_e} \frac{\partial}{\partial x} \delta P_g(x, t) \\ &\quad + \frac{e^2}{m_e} E_{\parallel}(x, t) [n_0 + \delta n_g(x, t)] \\ &\quad - \sum_{j=1}^N \frac{dw_j}{dt} (-e) v_{\parallel j} S(x - x_j), \end{aligned} \quad (23)$$

$$\begin{aligned} \frac{\partial}{\partial t} \delta P_g(x, t) &= -\frac{m_e v_t^2 b_x}{(-e)} \frac{\partial}{\partial x} \delta j_g(x, t) \\ &\quad + 2E_{\parallel}(x, t) [j_0 + \delta j_g(x, t)] \\ &\quad - \sum_{j=1}^N \frac{dw_j}{dt} m_e v_{\parallel j}^2 S(x - x_j), \end{aligned} \quad (24)$$

$$\delta n_g(x, t=0) = 0, \quad (25)$$

$$\delta j_g(x, t=0) = 0, \quad (26)$$

$$\delta P_g(x, t=0) = 0. \quad (27)$$

The  $\mathbf{E} \times \mathbf{B}$  drift in the  $x$  direction vanishes in the 1-dimensional model. The spatial derivatives are calculated

with the spectrum method. In the total characteristic simulation, the number density, current density, and pressure are given by

$$n(x, t) = n_0 + \delta n_K(x, t) + \delta n_g(x, t), \quad (28)$$

$$j(x, t) = \delta j_K(x, t) + \delta j_g(x, t), \quad (29)$$

$$P(x, t) = n_0 T_{e0} + \delta P_K(x, t) + \delta P_g(x, t). \quad (30)$$

### 3. Benchmarks on Kinetic Alfvén Wave

The real frequency and damping rate of the kinetic Alfvén wave for various electron beta values have been investigated with the simulation model described in the previous subsection. The physical parameters are the same as those used in Ref. [12],  $m_i/m_e = 1837$ ,  $k_{\perp}\rho_s = 0.4$ , and  $k_{\parallel}/k_{\perp} = b_{0x}/b_{0y} = 10^{-2}$  with  $b_{0z} = 0$ . The number of grid points is 64, the time step width  $\Delta t = 0.5\Delta x/b_{0x}v_t$ , and the number of Lagrangian markers  $N = 32768$ . The 4th-order Runge-Kutta method is employed for the time integration. The time step with the total characteristic method is restricted by the Courant condition for electrons. With regards to computational time, the total characteristic method requires additional computational time for the fluid equations, Eqs. (22)-(24). In the fluid equation calculation, the calculation of the terms with  $\sum_{j=1}^N \frac{dw_j}{dt} S(x - x_j)$  in Eqs. (22)-(24) demands the most computational time that is comparable to the calculation of  $\delta n_K$ ,  $\delta j_K$ , and  $\delta P_K$ . The calculation of  $\delta n_K$ ,  $\delta j_K$ , and  $\delta P_K$  often takes the longest time in the conventional  $\delta f$  simulations. Thus, the computational time with the total characteristic method is at most roughly twice that with the conventional  $\delta f$  method.

The real frequency and damping rate of the simulation results are compared with the theoretical values in Fig. 1. There is good agreement between the simulation results and theoretical values both for real frequency and damping

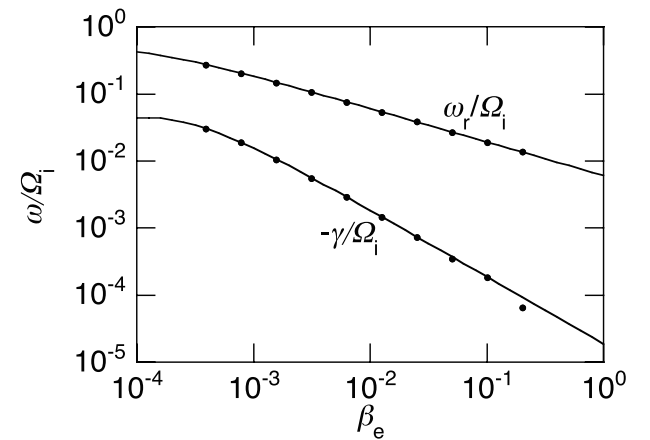


Fig. 1 Real frequency ( $= \omega_r$ ) and damping rate ( $= -\gamma$ ) of the kinetic Alfvén wave in the simulation results are plotted with closed circles for various electron beta values. Solid curves represent the theoretical frequencies.

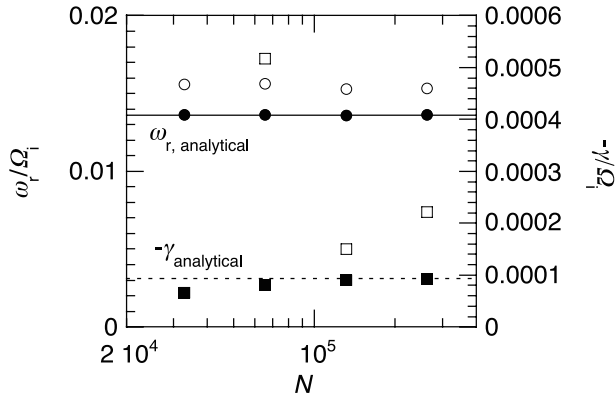


Fig. 2 Real frequency and damping rate versus number of marker particles. Solid line and dashed line represent analytical values of the real frequency and damping rate, respectively. Closed (open) circles and closed (open) squares represent the real frequency and damping rate in the simulation with the total characteristic method (with the conventional  $\delta f$  method).

rate. There is also good agreement for the low electron beta values ( $\beta_e < 10^{-3}$ ) for which the frequencies were not well reproduced with the hybrid method devised in Ref. [12] (see Fig. 1 of Ref. [12]). The theoretical frequencies of the kinetic Alfvén wave were calculated from Eq. (16) of Ref. [12] using a plasma dispersion function library DSPFNV [16]. In Fig. 1, the real frequency is roughly in proportion to the inverse of the square root of the electron beta. This can be explained as follows. The real frequency of the Alfvén wave in the fluid limit is given by  $k_{\parallel} B_0 / \sqrt{\mu_0 m_i n_0}$ . With the condition  $k_{\parallel} = 10^{-2} k_{\perp}$  and  $k_{\perp} \rho_s = 0.4$ ,  $k_{\parallel}$  is in proportion to the inverse of  $\rho_s$ . The ratio of the real frequency to the ion cyclotron frequency ( $= \omega_r / \Omega_i$ ) is in proportion to  $B_0 / \sqrt{\mu_0 m_i n_0 \rho_s \Omega_i} = B_0 / \sqrt{\mu_0 n_0 T_{e0}} = \sqrt{2/\beta_e}$ . Then, we have  $\omega_r / \Omega_i \propto \beta_e^{-1/2}$ .

In Fig. 1, we see a discrepancy in the damping rate between the simulation and theory for  $\beta_e = 0.2$ . For this case, the numerical convergence of real frequency and damping rate were investigated with respect to the number of marker particles using the total characteristic method and the conventional  $\delta f$  method. The results are compared in Fig. 2. It can be seen that the convergence with the total characteristic method is faster than with the conventional  $\delta f$  method. For  $N = 32768$  with the conventional  $\delta f$  method, the damping rate is  $-\gamma / \Omega_i = 1.6 \times 10^{-3}$  and is not shown in Fig. 2.

For the application to fusion plasmas, it is important to simulate with a grid size larger than the electron skin depth. For example, when the electron number density is  $10^{20} \text{ m}^{-3}$ , the electron skin depth is  $c/\omega_{pe} = 0.53 \text{ mm}$ . If two-hundred grid points are assigned for a 1m minor radius, the grid size is 5 mm, which is larger than the electron skin depth by one order of magnitude. Thus, it is important to simulate with a grid size larger than the electron

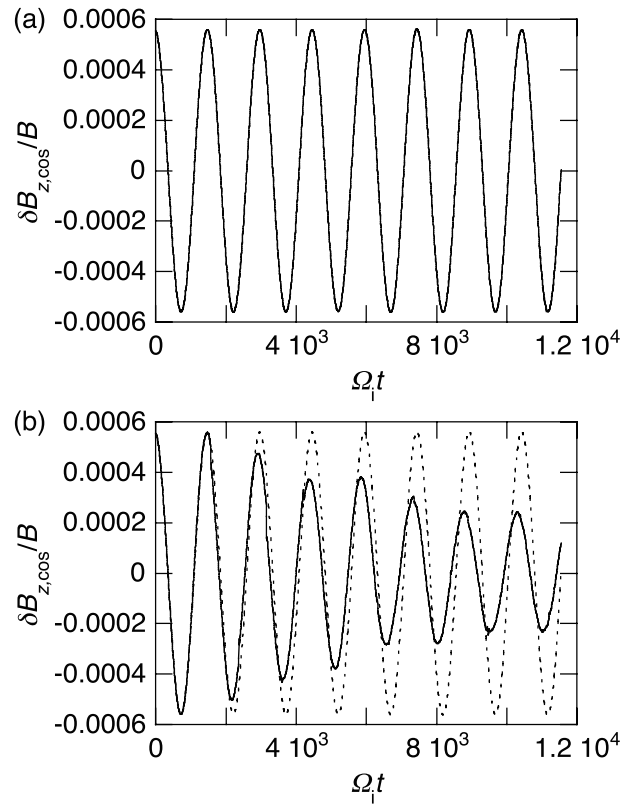


Fig. 3 Time evolution of the cosine part of  $B_z$  in simulations (a) with the total characteristic method and (b) with the conventional  $\delta f$  method are compared to the theoretical evolution plotted in dashed curves. The grid size is  $\Delta x = 10c/\omega_{pe}$ .

skin depth. We carried out a run with  $\Delta x = 10c/\omega_{pe}$  which is larger than the grid sizes for the runs shown in Fig. 1, for example,  $\Delta x = 0.15c/\omega_{pe}$  for  $\beta_e = 3.9 \times 10^{-4}$  and  $\Delta x = 3.3c/\omega_{pe}$  for  $\beta_e = 2.0 \times 10^{-1}$ . The physical parameters for the present run are  $m_i/m_e = 1837$ ,  $\beta_e = 10^{-2}$ ,  $k_{\perp} \rho_s = 3.0 \times 10^{-2}$ , and  $k_{\parallel}/k_{\perp} = b_{0x}/b_{0y} = 10^{-2}$ . The number of grid points is 64. The results are compared to those with the conventional  $\delta f$  method in Fig. 3. It can be seen that the results with the total characteristic method are close to the theoretical curve, while the kinetic Alfvén wave damps spuriously with the conventional  $\delta f$  method.

## 4. Summary

In this paper, we described how an electromagnetic plasma model is constructed with the total characteristic method. We demonstrated that both the real frequency and damping rate of kinetic Alfvén wave were computed correctly for various electron beta values. We found that with respect to the number of marker particles, the numerical convergence of the real frequency and damping rate with the total characteristic method is faster than with the conventional  $\delta f$  method. Specifically, we demonstrated that the total characteristic method enables a simulation of a

kinetic Alfvén wave with a grid size ten times larger than the electron skin depth, while the wave spuriously damps in the conventional  $\delta f$  simulation. The gyrokinetic simulation model with the total characteristic method presented in this paper is useful for magnetically confined plasmas such as tokamak plasmas and helical plasmas.

## Acknowledgments

The authors would like to thank Prof. T. Watanabe for the plasma dispersion function library DSPFNV. This work was supported by a Grant-in-Aid for Scientific Research from the Japan Society for the Promotion of Science (No. 16560728).

- [1] W.W. Lee, J. Comput. Phys. **72**, 243 (1987).
- [2] M. Kotschenreuther, Bull. Am. Phys. Soc. **33**, 2107 (1988).
- [3] A.M. Dimits and W.W. Lee, J. Comput. Phys. **107**, 309 (1993).
- [4] S.E. Parker and W.W. Lee, Phys. Fluids **B5**, 77 (1993).
- [5] A. Y. Aydemir, Phys. Plasmas **1**, 822 (1994).
- [6] H. Naitou, K. Tsuda, W.W. Lee and R.D. Sydora, Phys. Plasmas **2**, 4257 (1995).
- [7] Y. Chen and S.E. Parker, Phys. Plasmas **8**, 2095 (2001).
- [8] Y. Chen and S.E. Parker, J. Comput. Phys. **189**, 463 (2003).
- [9] W.W. Lee, J.L.V. Lewandowski, T.S. Hahm and Z. Lin, Phys. Plasmas **8**, 4435 (2001).
- [10] A. Mishchenko, R. Hatzky and A. Konies, Phys. Plasmas **11**, 5480 (2004).
- [11] Y. Chen and S.E. Parker, Phys. Plasmas **8**, 441 (2001).
- [12] Z. Lin and L. Chen, Phys. Plasmas **8**, 1447 (2001).
- [13] B.I. Cohen, A.M. Dimits, W.M. Nevins, Y. Chen and S.E. Parker, Phys. Plasmas **9**, 251 (2002).
- [14] Y. Todo, J. Plasma Fusion Res. **81**, 944 (2005), <http://www.jspf.or.jp/Journal/2005.html>
- [15] C.K. Birdsall and A.B. Langdon, *Plasma Physics via Computer Simulation* (Adam Hilger, Bristol, 1991) p. 393.
- [16] T. Watanabe, KAKUYUGO KENKYU **65**, 556 (1991) [*in Japanese*].